

## Response Site Analyses of 3D Homogeneous Soil Models

Davide Forcellini <sup>a\*</sup>, Marco Tanganelli <sup>b</sup>, Stefania Viti <sup>b</sup>

<sup>a</sup> *Università di San Marino, San Marino*

<sup>b</sup> *Università di Firenze, Italy*

### Abstract

The seismic excitation at the surface can be determined through Site Response Analyses (SRA) as to account for the specific soil properties of the site. However, the obtained results are largely affected by the model choice and setting, and by the depth of the considered soil layer. This paper proposes a refined 3D analytical approach, by the application of OPENSEES platform. A preliminary analysis has been performed to check the model adequacy as regards the mesh geometry and the boundary conditions. After the model setting, a SRA has been performed on various soil profiles, differing for the shear velocity and representing the different soil classes as proposed by the Eurocode 8 (EC8). Three levels of seismic hazard have been considered. The seismic input at the bedrock has been represented consequently, through as much ensembles of seven ground motions each, spectrum-compatible to the elastic spectra provided by EC8 for the soil-type A (bedrock). Special attention has been paid to the role of the considered soil depth on the evaluation of the surface seismic input. Different values of depth have been considered for each soil type and seismic intensity, in order to check its effect on the obtained results.

### Keywords:

Separated By Semicolons Response Site Analysis;  
Opensees;  
Numerical Simulations;  
Eurocode 8.

### Article History:

**Received:** 12 August 2018  
**Accepted:** 16 October 2018

## 1- Introduction

Seismic inputs assumed for the assessment of constructions subjected to seismic hazard are one of the most unpredictable quantities involved in the analyses. In particular, when nonlinear dynamic analyses are considered, two main issues need to be considered: the choice of the ground motions to use for analysis and the soil representation.

Both of these aspects have been widely investigated by researchers in the last decades. The main contributions regarding the ground motions selection pointed out the most important parameters, like the Magnitude [1], the distance from the rupture zone [2] and the soil profile [3] through a disaggregation approach [4]. Based on these main parameters, different procedures for Ground Motions Selection and Modification (GMSM) have been developed [5-10], based on Seismic Hazard Analysis [4, 11], which attributes a multivariate distribution to the considered classification accounting for the marginal probability of the optimization function.

In addition, soil representation plays a crucial role in the seismic assessment of buildings. Most of the International Technical Codes, like Eurocode 8 [12], ASCE standards 7-05 [13] and 4-98 [14], provide seismic spectra defined after a proper soil classification, which is usually based on the uppermost 30 m shear-wave velocity ( $v_{s,30}$ ) of the site.  $v_{s,30}$  can be determined through different geological investigations [15-19] and it can largely vary even within the same area [20, 21]. Sometimes, the limit of 30 meters for the soil characterization can be not completely adequate, since deepest layers of soil can still affect the surface seismic input [22-24]. Furthermore, a soil characterization based on average values of the mechanical parameters is not always conservative. In this regard, recent studies [25] showed that when superficial deposit lays over the bedrock, amplification of surface seismic accelerations can evidence unexpected peaks at the deposit edges, where the thickness of the deposit is lower. In these cases, averaging the soil properties over the uppermost 30 meters can induce to un-conservative results.

When SRA are related with extensive investigations on the soil mechanical properties, more affordable evaluation

\* **CONTACT:** [davforc@omniway.sm](mailto:davforc@omniway.sm)

**DOI:** <http://dx.doi.org/10.28991/esj-2018-01148>

© This is an open access article under the CC-BY license (<https://creativecommons.org/licenses/by/4.0/>).

of the surface seismic input can be obtained. Previous investigations [20, 21, 26, 27] showed that the surface seismic input can largely differ from the one provided by the Code for the corresponding soil-class. However, the seismic input obtained by performing a SRA is affected by several different assumptions, including the soil modeling, the description of its mechanical properties, and the analytical procedure to use for the analysis.

This paper adopts a refined 3D analytical approach, through the OPENSEES platform. A SRA has been performed on different homogeneous soil profiles, differing for the shear velocity and cohesion and representing the different soil classes as proposed by the Eurocode 8 (EC8). Three different seismic intensities (corresponding to a value of PGA equal to 0.15, 0.25 and 0.35 g) have been considered in the analysis, in order to check RSA sensitivity to inelastic soil properties. The seismic input at the bedrock has been represented through an ensemble of seven ground motions, whose *mean* is spectrum-compatible to the elastic spectrum provided by EC8 for the soil-type A (bedrock). Special attention has been paid to the effect of soil depth on the evaluation of the surface seismic input. Different values of depth have been considered for each soil type and seismic intensity, in order to check its effect on the obtained results.

## 2- Seismic Input at the Bedrock

### 2-1-The Current Code Classification

In Figure 1 the soil classification respectively provided by the European EC8 and the Italian NTC 2008 have been shown and compared to the one proposed by Pitilakis et al. (2013) [28]. As can be noted, the EC8 and NTC 2008 [29] classification differ each other mostly for the condition regarding the soil depth ranging between 20 m and 30 m. The Italian classification, indeed, introduces the soil-type S2, which collects all the soil profiles not covered from the other classes. The classification proposed in [28] adopts a classification similar to the EC8 one, dividing some of the classes in further sub-classes, defined by introducing further parameters (like the fundamental period of the soil). Figure 1 represents the sub-classes belonging to the same main class with the same color and different patterns. The elastic spectra representing the soil classes according to each classification differ each other for shape and definition of the reference periods.

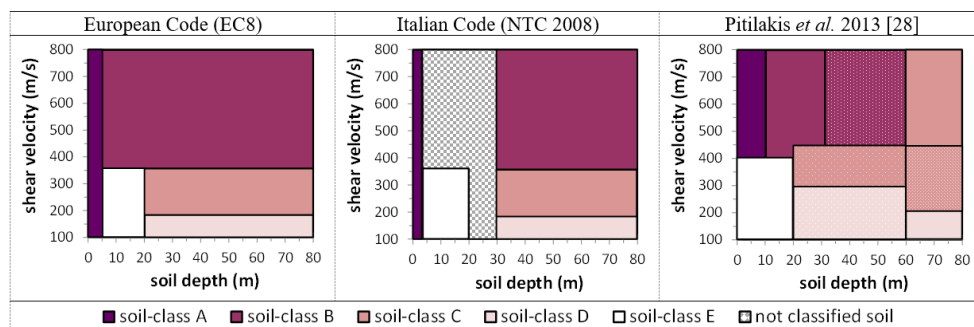


**Figure 1.** Soil classification according to the European (EC8) and Italian (NTC 2008) classification and the Pitilakis et al. 2013 [28] proposal.

### 2-2- Seismic Input at the Bedrock

This paper considers three different seismic intensities with PGA values respectively equal to 0.15, 0.25 and 0.35 g. For each intensity, the seismic input at the bedrock has been represented through an ensemble of 7 ground motions, spectrum-compatible to the elastic spectrum representing the rock (soil-class A). The different Codes provide for the A-soil an elastic spectrum slightly different. Namely, the Italian Code NTC 2008 provides spectra whose shape depends on the considered seismic intensity. In Table 1 the main parameters defining the elastic spectra of the soil-type A according to EC8, NTC 2008 and Pitilakis et al. (2013) proposal are listed. In Figure 2 their elastic spectra are shown for the three considered intensities. The reference periods describing the NTC 2008 spectrum refer to specific Italian sites, since they depend on site-specific parameters. In this paper, EC8 has been assumed as reference Code for the seismic input definition. Ground motions have been selected by the database Itaca [30] through the software Roxel [31]. For each PGA, a proper ensemble of ground motions has been considered, in order to use unscaled records. In Table 2 the main information of the assumed records are listed, and the comparison between each ensemble and the corresponding EC8 elastic spectrum has been shown. Figure 3 shows the ratio between the mean spectrum of each considered ensemble and the corresponding EC8 one. As can be noted, the scatter between the considered ensembles and the corresponding EC8 spectrum keeps below -10% to +30%, except for few periods around 0,1 sec, i.e. out of the range of interest (0.2 -2.0 sec) required by the Code.

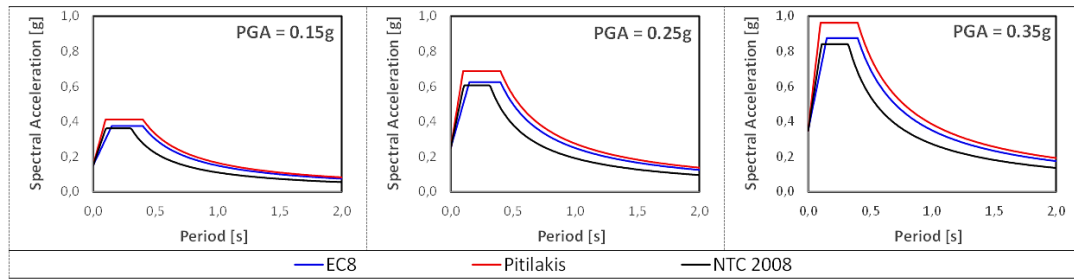


Figure 2. Elastic spectra of the soil-type A.

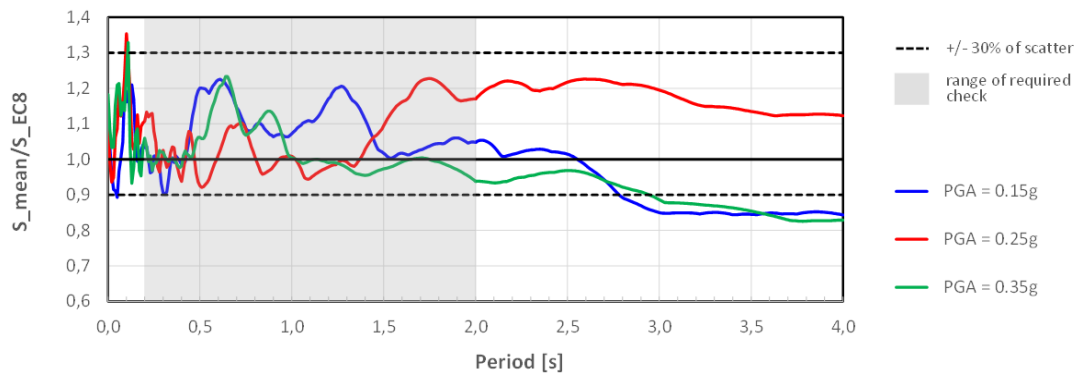


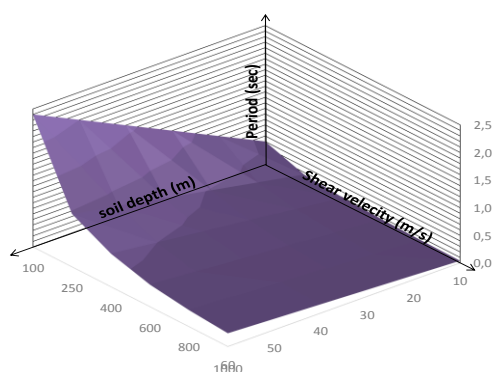
Figure 3. Comparison between the mean spectrum of the three ensembles and the corresponding EC8 ones.

Table 1. Reference data for the spectrum of the soil-type A.

EC8					NTC 2008					Pitilakis et al. 2011						
T <sub>B</sub>	T <sub>C</sub>	T <sub>D</sub>	S	PGA	Site	CU, ls	F <sub>0</sub>	T* <sub>c</sub>	T <sub>B</sub>	T <sub>C</sub>	T <sub>D</sub>	T <sub>B</sub>	T <sub>C</sub>	T <sub>D</sub>	S	β
				0.15	Firenze	III, LS	2.409	0.306	0.10	0.30	2.20					
00.15	0.40	2.00	1.00	0.25	Arezzo	IV, LS	2.424	0.316	0.10	0.31	2.60	0.10	0.40	2.00	1.00	2.75
				0.35	Sansepolcro	IV, CP	2.401	0.324	0.10	0.32	3.00					

### 3- Assumed Soil Profiles

Six soil types have been considered in this paper, with different values of shear velocity ( $V_s$ ) and cohesion ( $C$ ), in order to represent the range of possible types considered in the Code classification. Table 3 shows the considered soil types (which have been named after their values of  $V_s$ ) together with the main parameters assumed for their description. Six different depth values, ranging between 10 and 60 m, have been considered in the analysis, with the aim to check the role of this parameter on the surface input definition. According to the main Codes, indeed, the soil characterization is made after the uppermost 30 m shear velocity ( $V_{s,30}$ ). This means that usually the investigations on the soil are aimed at checking the uppermost 30 meters only. The effect of the soil depth on its elastic fundamental period has been preliminary checked. The elastic periods, shown in Figure 4, have been found by the formulation expressing the elastic wave propagation:  $T = 4 H / V_s$  [32], where  $H$  is the height of the soil layer.



Soil type	Considered depth of the soil					
	10m	20m	30m	40m	50m	60m
Vs_100	0.40	0.80	1.20	1.60	2.00	2.40
Vs_250	0.16	0.32	0.48	0.64	0.80	0.96
Vs_400	0.10	0.20	0.30	0.40	0.50	0.60
Vs_600	0.07	0.13	0.20	0.27	0.33	0.40
Vs_800	0.05	0.10	0.15	0.20	0.25	0.30
Vs_1000	0.04	0.08	0.12	0.16	0.20	0.24

Figure 4. Elastic periods of the considered soils.

**Table 2. Adopted ground motions.**

PGA = 0.15g (low seismicity, L)						Spectral Acceleration [g]	Period [s]
Code	event	date	station	PGA	Mg		
L_1	Umbria-Marche	09/26/1997	CSA	0.172	5.8		
L_2	Friuli	09/15/1976	GMN	0.255	6		
L_3	Abruzzo	05/07/1984	CNS0	0.113	5.9		
L_4	Emilia	05/29/2012	MIRH	0.150	6		
L_5	Emilia	05/29/2012	T0811	0.193	6		
L_6	Emilia	05/29/2012	T0818	0.161	5.5		
L_7	Emilia	05/29/2012	T0824	0.145	6		
PGA = 0.25g (medium seismicity, M)						Spectral Acceleration [g]	Period [s]
Code	event	date	station	PGA	Mg		
M_1	Emilia	05/29/2012	BA	0.177	5.8		
M_2	Friuli	09/15/1976	GMN	0.255	6		
M_3	Emilia	05/29/2012	MIR	0.217	5.8		
M_4	Emilia	05/20/2012	MRN01	0.262	5.9		
M_5	Emilia	05/29/2012	MRN02	0.223	5.8		
M_6	Emilia	05/29/2012	T0814	0.505	5.8		
M_7	Emilia	05/29/2012	T0819	0.259	5.3		
PGA = 0.35g (high seismicity, H)						Spectral Acceleration [g]	Period [s]
Code	event	date	station	PGA	Mg		
H_1	Abruzzo	06/04/2009	AQG	0.446	5.9		
H_2	Abruzzo	06/04/2009	AQV01	0.657	5.9		
H_3	Abruzzo	06/04/2009	AQV02	0.546	5.9		
H_4	Emilia	05/20/2012	MRN01	0.262	5.9		
H_5	Emilia	05/29/2012	MRN03	0.294	5.8		
H_6	Emilia	05/29/2012	MIR08	0.248	5.8		
H_7	Emilia	05/29/2012	T0814-01	0.445	5.8		

**Table 3. Assumed soil types.**

Soil types	Vs_100	Vs_250	Vs_400	Vs_600	Vs_800	Vs_1000
Reference EC8 soil-type	D/E	C/E	B	B	B	A
Mass density (kN/ m <sup>3</sup> )	1.5	1.5	2	2	2	2
Poisson	0.4	0.4	0.4	0.4	0.4	0.4
Shear Wave Velocity, $v_s$ (m/s)	100	250	400	600	800	1000
Cohesion, $C$ (kPa)	70	250	350	425	500	800
Peak Shear Strain	3	3	3	3	3	3
Number of Yield Surface	20	20	20	20	20	20

#### 4- FEM Model

The finite element method (FEM) model has been built with OpenSees [33] that allows high level of advanced capabilities for modelling and analysing non-linear responses of systems using a wide range of material models, elements and solution algorithms. In particular, this platform consists of a framework for saturated soil response as a two-phase material following the u-p (where u is displacement of the soil skeleton and p is pore pressure) formulation. This interface, which had been originally calibrated for pile analysis, it has been modified in this study by eliminating the pile elements in order to consider a free field case study. The model applies hysteretic elasto-plastic materials in order to take into account realistic behaviour of the soil, modified by the degradation of soil stiffness and energy dissipation. Soil damping has been modelled by considering a nonlinear material [34, 35], which takes into account the dynamic nature of the phenomena (such as hysteretic response and radiation damping). In particular, the damping is not

predefined by the user with a value as many numerical platforms do, but it is directly computed by the implemented materials (including permanent deformations and damping foundation impedances).

Plasticity is formulated based on the multi-surface (nested surfaces) concept, with an appropriate non-associative flow rule [36-40]. The nonlinear shear stress strain back-bone curve is represented by a hyperbolic relationship [41], defined by the two material constants: the low-strain shear modulus and the ultimate shear strength. Soil has been modelled with four clay materials called Pressure Independent Multiyield [33] built up with the representative parameters shown in Table 3. In order to introduce these parameters inside the code, the shear strain - shear stress relationships (backbone curves) have been implemented. Figure 4 shows the applied curves for the considered soils.

In addition, OpenSees simulates real wave propagation by adopting realistic boundaries that have been located as far as possible from the structure as to decrease their effects on the response. In particular, at any special location, symmetry conditions can be adopted and periodic boundaries [42] have been considered. Displacement degrees of freedom of the left and right boundary nodes have been tied together both longitudinally and vertically using the penalty method. In this regard, base and lateral boundaries have been modelled to be impervious, as to represent a small section of a presumably infinite (or at least very large) soil domain and allowing the seismic energy to be removed from the site itself. For more details, see Elgamal et al. 2009 [43], Forcellini and Gobbi 2015 [44] and Forcellini 2017 [45]. The 3D mesh aims at performing tridimensional SRA analyses, by applying OpenSees potentialities. Based on previous studies [44, 45], the soil has been considered a one-layer homogenous cohesive material and consisting in 3D FE meshes (plan area:  $150.0 \times 37.5$  m) composed of brickUP linear isoparametric 8-nodes elements [33].

Mesh dimensions have been determined between 0.125 to 0.027 times of the Rayleigh wavelength, in according with the suggestions indicated in Attewell and Farmer (1973) [46] and Jesmani et al. (2012) [47] and based on Rayleigh wavelength and already applied in [45, 48, 49]. Furthermore, a preliminary calibration analysis has been performed, which included a number of nodes ranging between 396 and 3585. The assumed final mesh, represented in Figure 5, has 36 elements for each layer, and a different number of vertical layers (8, 10, 14, 18 and 18, respectively) depending on the considered depth, with homogeneous heights. Discretization is built up with relatively small elements around the centre and gradually larger toward the outer mesh boundaries, by increasing the distance from the mesh outer edge. In particular, at any special location, symmetry conditions can be adopted and periodic boundaries [42] have been considered.

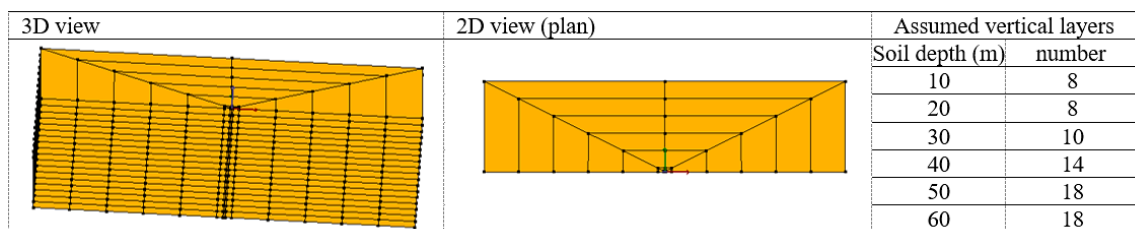


Figure 5. FEM model adopted in the analyses.

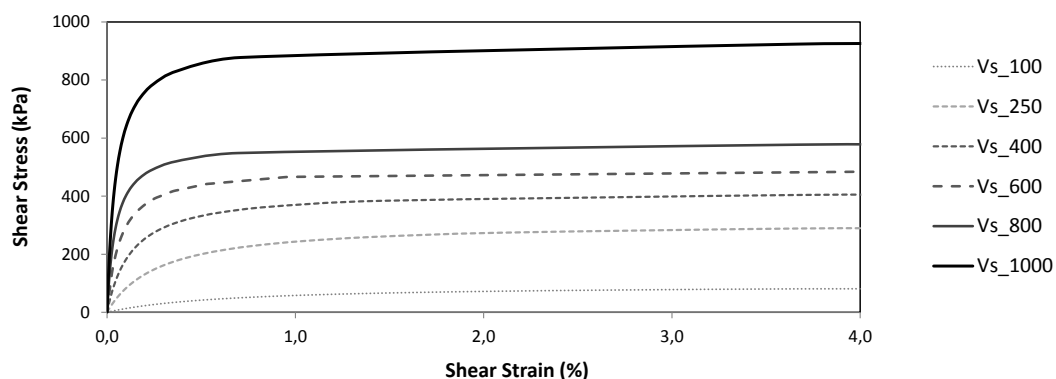


Figure 6. Backbone curves of the considered soil types.

## 5- RSA Analyses

The surface spectra have been found by performing SRA with the assumed seismic inputs at the bedrock through the assumed soil models.

Figure 7 shows the obtained mean spectral acceleration found for the three considered PGAs. The effects of the considered soil depth vary significantly in correspondence with the considered soil types. When the thinnest layer is



considered (soil depth equal to 10m), the surface acceleration experiences a large increase for soft soils ( $V_{s\_100}$ ,  $V_{s\_250}$ ,  $V_{s\_400}$ ). The increase is more moderate for the stiffer soil types. The 20 m layer achieves its maximum increase for medium soils ( $v_s$  between 400 and 800 m/s), whilst the thicker layers (30, 40, 50, 60 m) experience larger surface acceleration for stiffer soils. The largest surface accelerations, slightly below 4.0g, are achieved for the highest PGA value ( $PGA = 0.35g$ ), for different values of soil depths: depth equal to 10m ( $V_{s\_250}$ ,  $V_{s\_400}$ ), to 20 m ( $V_{s\_600}$ ,  $V_{s\_800}$ ) and to 40 m ( $V_{s\_1000}$ ).

Figure 8 shows the effects of soil depth and stiffness in terms of amplification functions (defined as the ratio between the surface spectrum and the corresponding spectrum at the bedrock) provided by the analysis and compared to the EC8 corresponding ones. These last functions have been found as the ratio between the elastic spectra provided by EC8 for the soil-type representing each considered soil, as evidenced in Table 3, and the A-soil one.

Figure 9 shows the results of this comparison, expressed in terms of  $FA/AF_{EC8}$ . Values exceeding the unity express an underestimation of the Code, regarding the amplification induced by the soil. In Figures 7-9, the highest amplification factors occur for the lowest PGA, when the soil is not involved by inelastic behaviour. The soil models belonging to the classes C, D and E ( $V_{s\_100}$ ,  $V_{s\_250}$ ) evidence the largest amplifications for periods bigger than 1.5 sec. This effect can be detrimental particularly for tall buildings. The most common types of existing RC buildings (which a number of storeys ranging between 3.0 and 6.0) should not significantly be affected.

However, for layers of soft soil with low thickness (10, 20 m), high values of amplification (exceeding value of 4) can be observed. This result confirms the evidence found in recent research on seismic engineering, regarding peaks of acceleration at the ends of superficial sediment, where the thickness is lower. Stiffer soils ( $V_{s\_400}$ ,  $V_{s\_600}$ ,  $V_{s\_800}$ ), instead, classified as B-class according to the EC8 classification, present the maximum amplification for periods below 0.5 sec, compatible with the fundamental periods of typical residential buildings. The maximum amplification achieves the value of 3 for the highest seismicity, whilst it ranges between 4.0 and 5.0 for lower PGAs, due to the elastic response of the soil. Finally, the stiffer considered soil ( $V_{s\_1000}$ ), classified as A-class according to EC8, evidences high values of the amplification function, not considered in EC8, for low periods (below 0,3 sec) ranging between 4.0 and 6.0 depending on the considered PGA.

Figures 10 and 11 show the surface acceleration and the amplification function in a 3D view, as a jointed function of the soil depth and shear velocity. Figure 12 shows a 3D view of the periods at the maximum amplification as a function of the depth and shear velocity. As can be noted, comparing the period surface to the one shown in Figure 4, representing the periods corresponding to the elastic wave propagation, the period surface evidences a similar trend for all cases, whilst the values of the periods increase at the inelastic involvement of the soil stress, i.e. at the increasing of the seismic input.

## 6- Conclusion

This paper presents SRA on different soil models, differing both for mechanical properties and consequent EC8 classification, and depth, by using a 3D FEM non-linear platform (OpenSees). Six different soils (with  $v_{s,30}$  between 100 and 1000 m/s and  $C$  between 70 and 800 kPa) and six different depth values (ranging between 10m and 60m) have been performed in the analyses. Three different seismic intensities have been considered ( $PGA$  equal to 0.15, 0.25 and 0.35 g). For each assumed intensity, an ensemble of 7 unscaled ground motions (spectrum-compatible to the EC8 elastic A-soil spectrum) have been selected. The mean surface acceleration has been compared to the mean spectrum at the bedrock, in order to evaluate the properties of the Amplification Function.

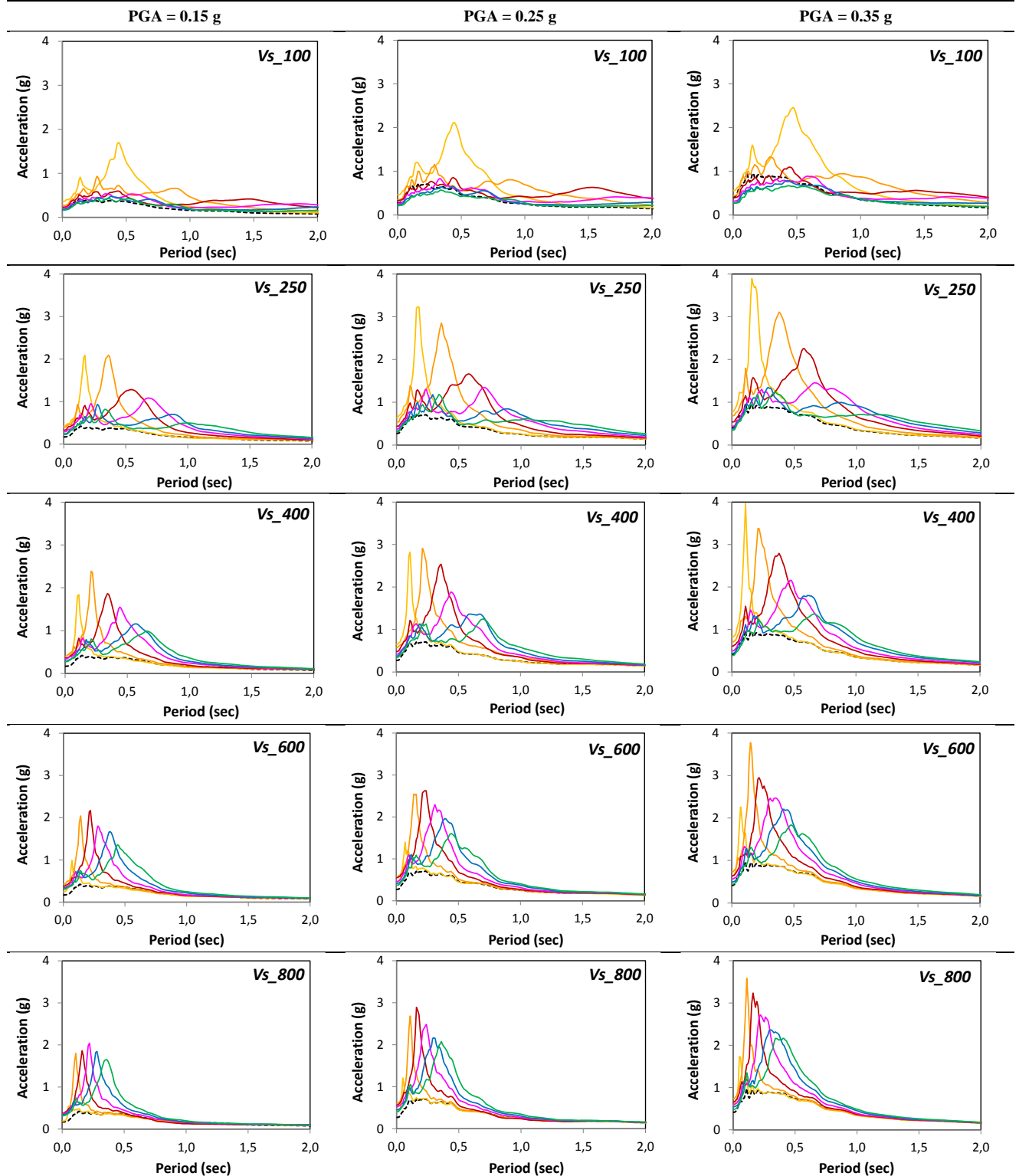
Several results have been deduced. First of all, the effects of the soil inelasticity. At the increasing of the  $PGA$ , indeed, soil amplification decreases, whilst the period corresponding to the maximum amplification does not seem to significantly sensitive to soil inelasticity. As regards the effects of the considered soil depth on the amplification factor, different trends have been observed for the considered soil types. The soil models belonging to the classes C, D and E ( $V_{s\_100}$ ,  $V_{s\_250}$ ) evidence the maximum amplification, ranging between 2.0 and 4.0 depending on the considered  $PGA$ , in correspondence with periods over 1.5 sec (out of the range of period of interest for the many existing buildings). For thin layers of soft soil (10 m), however, high values of amplification (around 5.0), can be observed for period equal to 0.5 sec, that is a value of large interest for existing buildings. This result confirms the evidence found in recent researches, regarding peaks of acceleration at the ends of superficial sediment (in correspondence with low thickness). In all cases, the amplification functions provided by the analyses are significantly higher than the EC8 ones.

Medium stiff soils ( $V_{s\_400}$ ,  $V_{s\_600}$ ,  $V_{s\_800}$ ) and classified as B-class according to the EC8, show the maximum amplifications for Periods below 0.5 sec. Maximum amplification achieves the value of 2.5-4.0 (depending on the soil depth) for the highest seismicity, whilst it ranges between 3.5 and 6.0 for lower  $PGA$ . Even in this case, the amplification found by performing the SRA, is much higher than the one provided by EC8.

The stiffer soil ( $V_{s\_1000}$ ), classified as A-class (according to EC8), evidences negligible amplification functions for periods over 0.5 sec, while the bedrock records experience large amplifications (between 3 and 5 times the bedrock

ones) for lower periods, whose interval is smaller (0.1-0.3 sec) for lower seismicity (PGA=0.15g) and slightly larger (0.1-0.5 sec) for higher one (PGA=0.35 g).

In conclusion, the research evidences the sensitivity of the surface seismic input to the assumed soil depth. In medium-consistent soils (belonging to the B-class), soil depth affects mainly input amplification. The period corresponding to the amplification peak, has been shown to be affected. In softer soils, (belonging to C, D and E classes), soil depth affects the period corresponding to the amplification peak more than the amplification amount. The analysis has evidenced a relevant peak in the amplification for soft soil with low depth, confirming the phenomena occurred in recent earthquakes. The soil depth resulted to be significant for the evaluation of the surface seismic input. Further studies will investigate multiple-layered soil models.



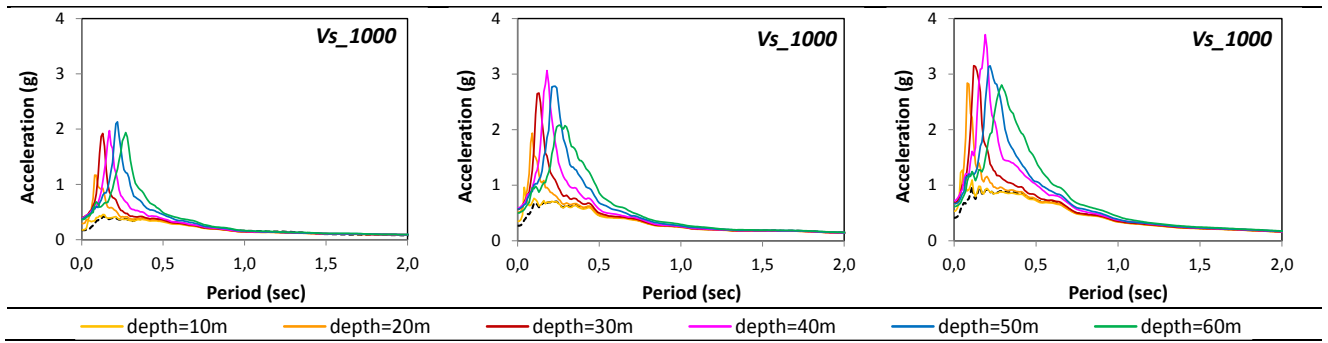
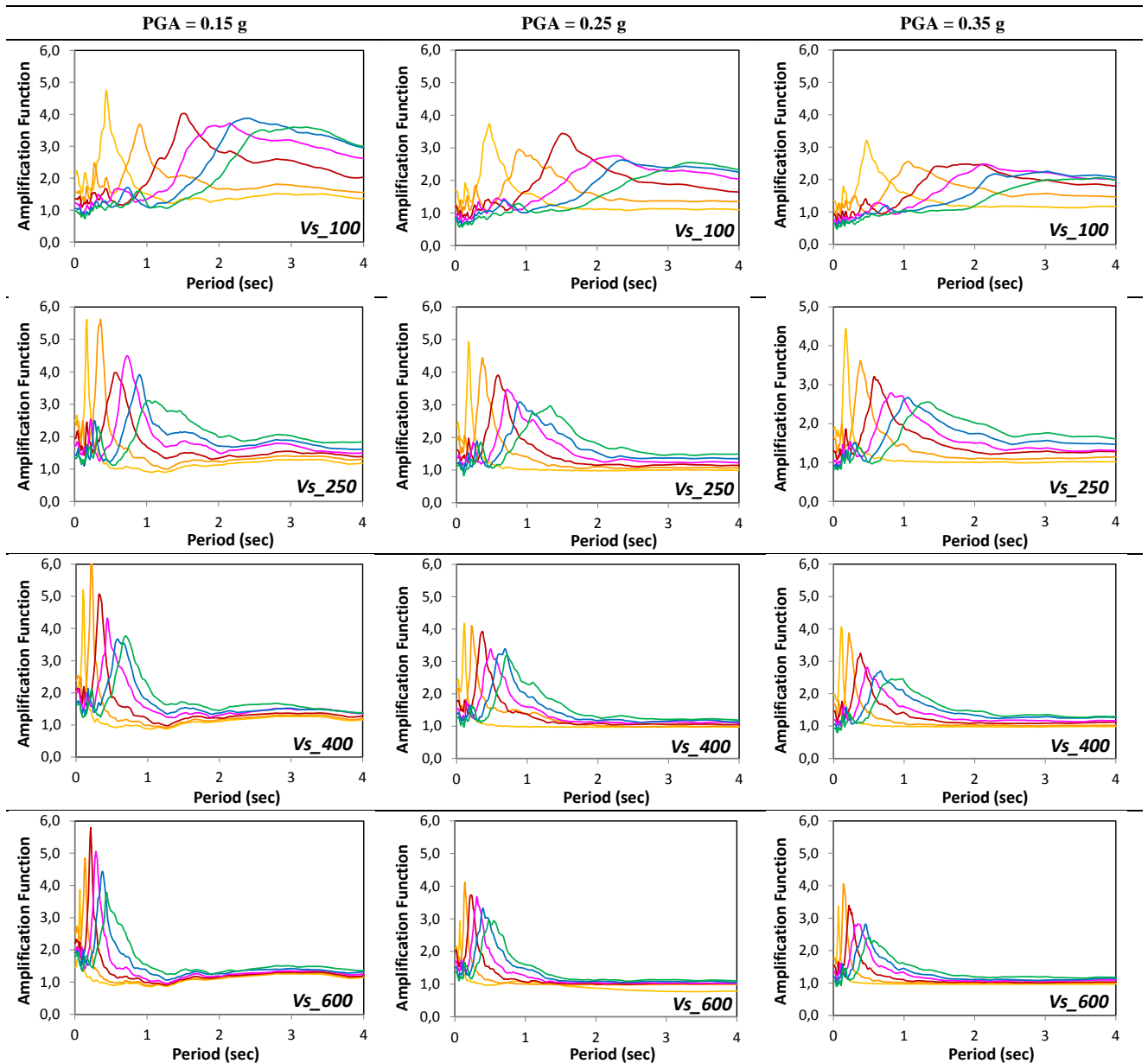


Figure 7. Surface spectral acceleration found through the SRA.





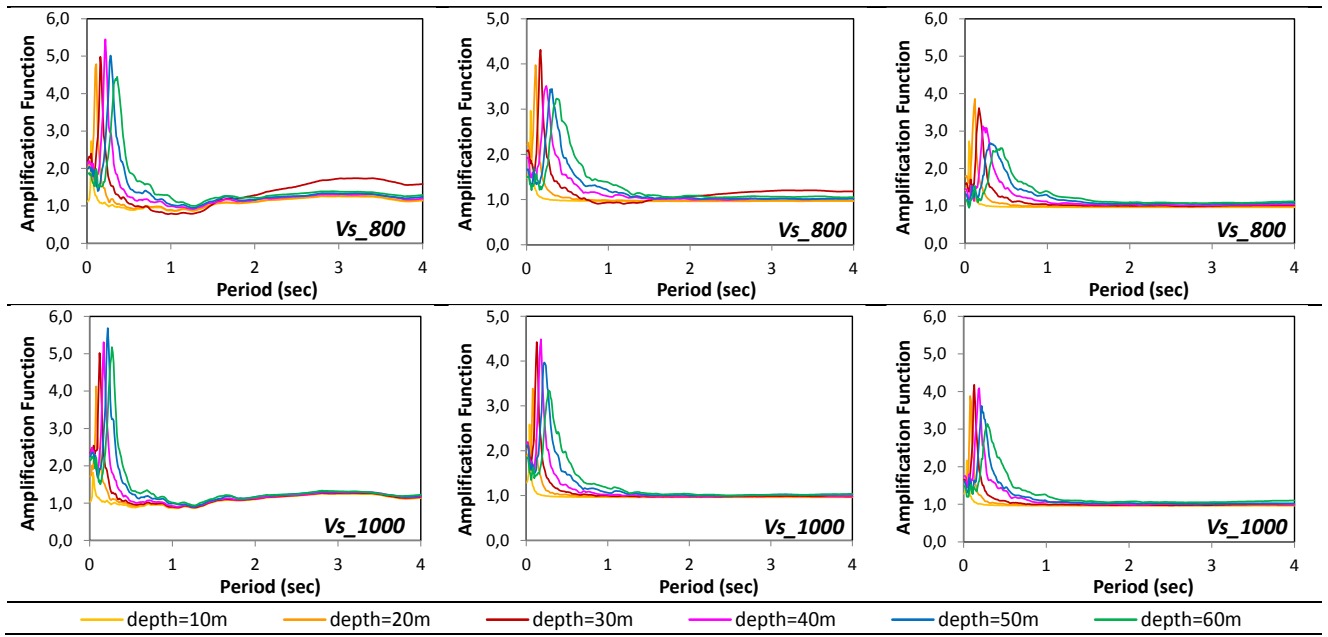
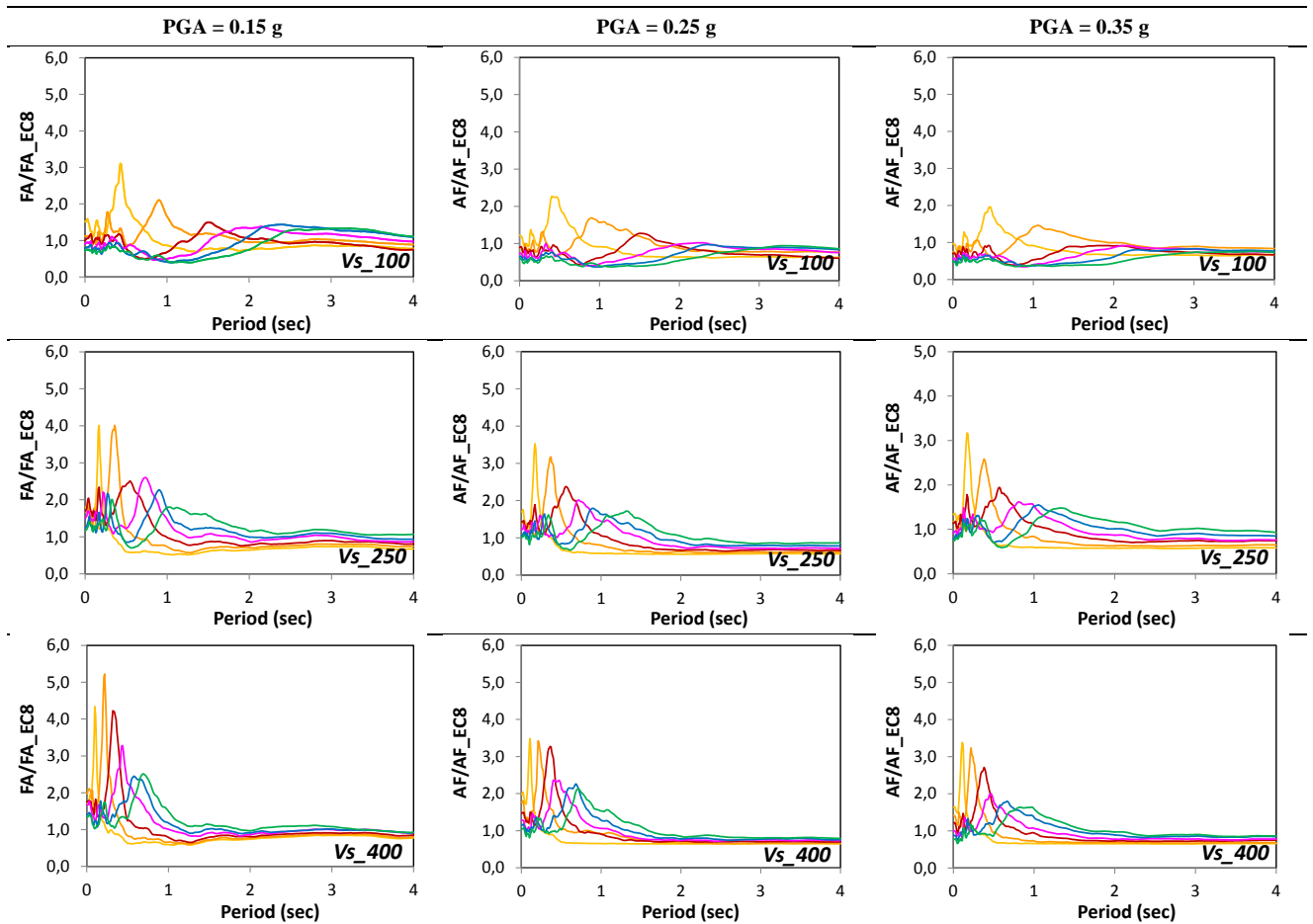


Figure 8. Amplification Functions.



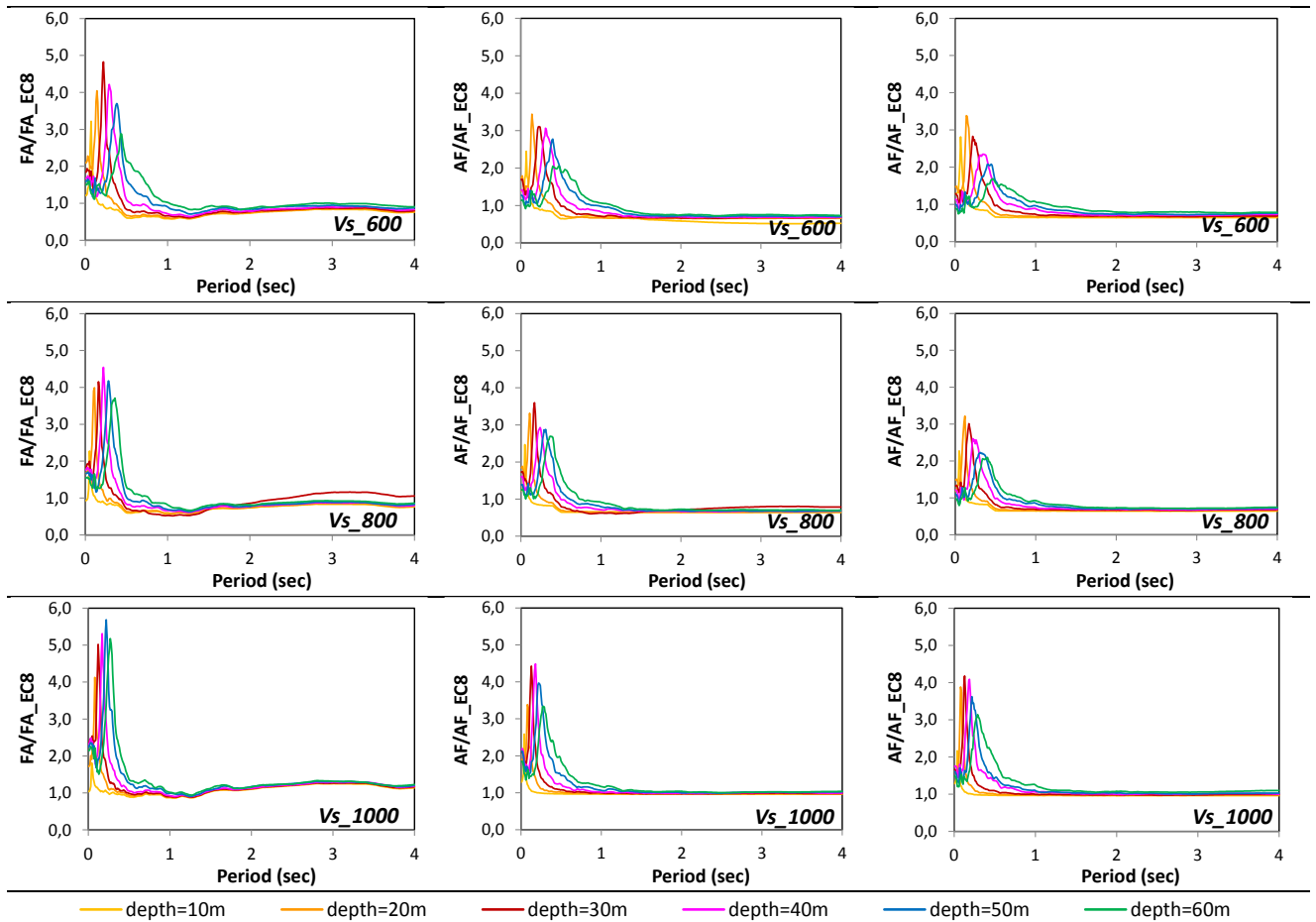


Figure 9. Ratio between FA provided by the analysis and the EC8 ones.

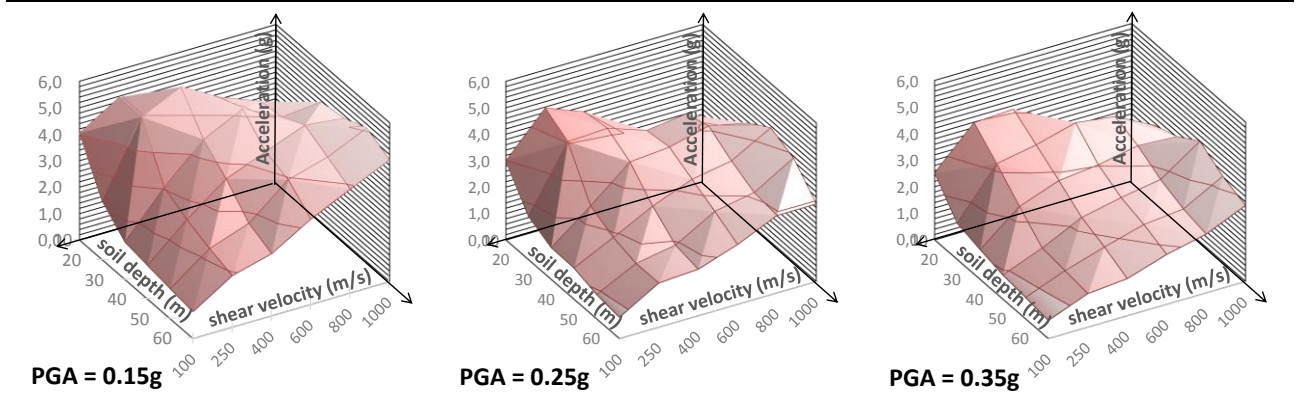


Figure 10. 3D view of the surface spectral acceleration.

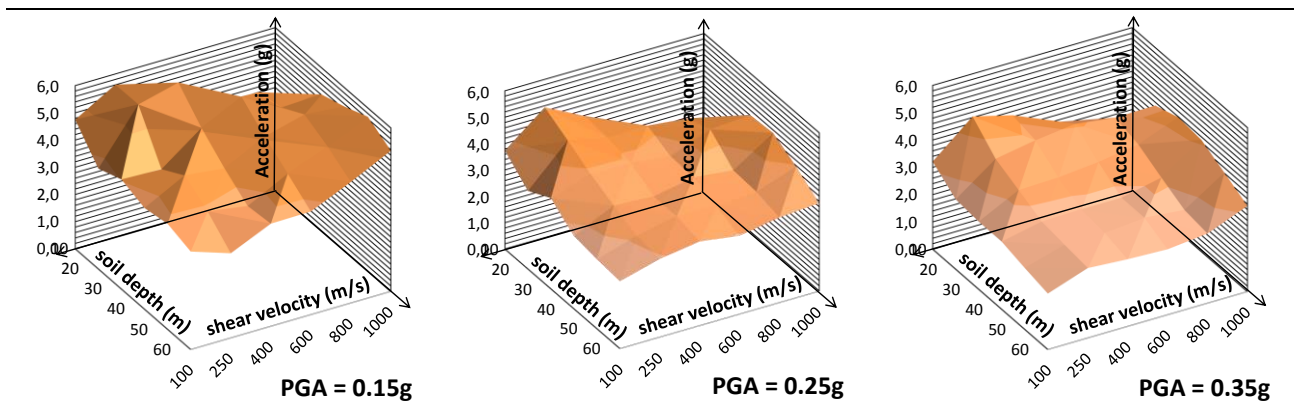
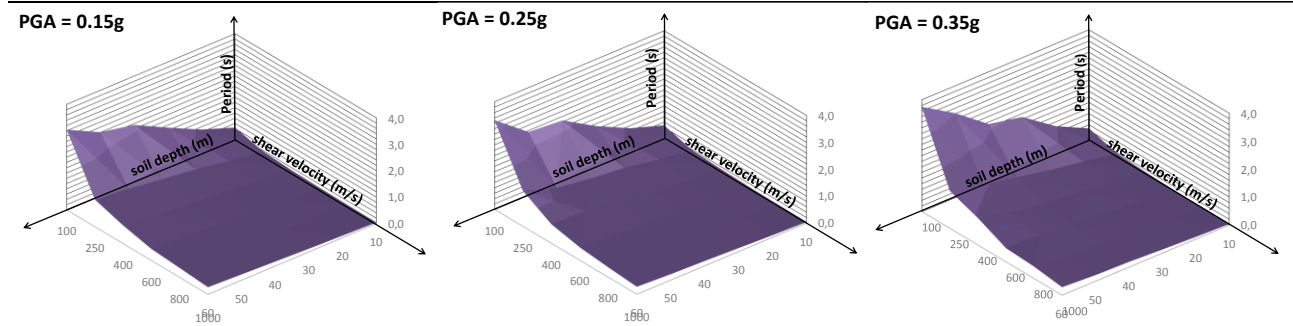


Figure 11. 3D view of the Amplification Function.



**Figure 12. 3D view of the Period at the maximum amplification.**

## 7- References

- [1] Shome N, Cornell CA, Bazzurro P, Carballo JE (1998). Earthquakes, records and nonlinear responses. *Earthq Spectra* 14(3):469–500
- [2] Stewart JP, Chiou SJ, Bray JD, Graves RW, Somerville PG, Abrahamson NA (2001). Ground motion evaluation procedures for performance-based design. Technical Report, PEER Center: University of California, Berkeley.
- [3] Bommer JJ, Acevedo A (2004). The use of real earthquake accelerograms as input to dynamic analysis. *Journal of Earthquake Engineering* 8 (sup001), pp. 43–91. doi: 10.1080/13632460409350521
- [4] Bazzurro P, Cornell CA (1999). Disaggregation of seismic hazard. *Bull Seismol Soc Am* 89 (2), pp. 501–520, Print ISSN 0037-1106
- [5] Katsanos EI, Sextos AG, Manolis GD (2010). Selection of earthquake ground motion records: a state-of-the-art review from a structural engineering perspective. *Soil Dynamic & Earthquake Engineering* 30 (4), pp. 157–169. doi: 10.1016/j.soildyn.2009.10.005.
- [6] Tarbali K, Bradley BA (2015). Ground motion selection for scenario ruptures using the generalized conditional intensity measure (GCIM) method. *Earthq Eng Struct Dyn* 44 (10), pp. 1601–1621. doi: 10.1002/eqe.2546.
- [7] Iervolino I, Chioccarelli E, Convertito V (2011). Engineering design earthquakes from multimodal hazard disaggregation. *Soil Dyn Earthq Eng* 31 (9), pp. 1212–1231. doi: 10.1016/j.soildyn.2011.05.001.
- [8] Al Atik L, Abrahamson N (2010). An improved method for nonstationary spectral matching. *Earthq Spectra* 26 (3), pp. 601–617. doi: 10.1193/1.3459159.
- [9] Seifried AE, Baker JW (2014). Spectral variability and its relationship to structural response estimated from scaled and spectrum-matched ground motions. In: *Proc. 10NCEE, Anchorage, Alaska, July 21–25, 2014.*
- [10] Bradley BA (2010) A generalized conditional intensity measure approach and holistic ground-motion selection. *Earth Eng Struct Dyn* 39 (12), pp. 1321–1342. doi: 10.1002/eqe.995
- [11] Baker JW (2011), Conditional mean spectrum: tool for ground motion selection. *ASCE J Struct. Eng.* 137 (3), pp. 322–331. doi: 10.1061/(ASCE)ST.1943-541X.0000215.
- [12] EC 8-3 (2005) Design of structures for earthquake resistance, part 3: strengthening and repair of buildings. European standard EN 1998-3. European Committee for Standardization (CEN), Brussels
- [13] ASCE (2006), Minimum design load for buildings and other structures. ASCE standard no. 007-05, American Society of Civil Engineering.
- [14] ASCE (2000), Seismic analysis of safety-related nuclear structures and commentary. ASCE standard no. 004-98, American Society of Civil Engineering.
- [15] Foti S, Parolai S, Albarello D, Picozzi M (2011). Application of Surface-Wave Methods for Seismic Site Characterization. *Surv Geophys* 32 (6), pp. 777–825. doi: 10.1007/s10712-011-9134-2.
- [16] Stokoe KH, Nazarian S, Rix GJ, Sánchez-Salinerio I, Sheu JC and Mok YJ (1988). In Situ Seismic Testing of Hard-to-Sample Soils by Surface Wave Method, *Earthquake Engineering and Soil Dynamics II - Recent Advances in Ground Motion Evaluation*, ASCE Geotechnical Special Publication No. 20, J.L. Von Thun, Ed., pp. 264-278.
- [17] Amorosi, A., Castellaro, S., Mulargia, F. (2008), “Single-Station Passive Seismic Stratigraphy : an inexpensive tool for quick subsurface investigations”, *GEOACTA*, 2008, 7, pp. 29 – 39.

- [18] Hobiger M, Wegler U, Shiomi K, Nakahara H (2014). Single-station cross-correlation analysis of ambient seismic noise: application to stations in the surroundings of the 2008 Iwate-Miyagi Nairiku earthquake. *Geophysical Journal International*, 198 (1): pp. 90-109. doi: 10.1093/gji/ggu115.
- [19] Wair BR, DeJong JT (2012). Guidelines for Estimation of Shear Wave Velocity Profiles. PEER Report 2012/08.
- [20] Tanganelli M, Viti S, Forcellini D, D'Intinsonante V, Baglione M (2016). Effect of soil modeling on Site Response Analysis (SRA). *Proc. SEMC 2016, Cape Town, South Africa, 5 - 7 September 2016*, Alphose Zingoni, vol. Insights and Innovations in Structural Engineering, Mechanics and Computation, pp. 364-369, ISBN:978-1-138-02927-9.
- [21] Viti S, Tanganelli M, D'Intinosante V, Baglione M (2017). Effects of soil characterization on the seismic input. *Journal of Earthquake Engineering* 21(6). doi: 10.1080/13632469.2017.1326422.
- [22] Assimaki D, Kausel E and Gazetas G (2005), Soil-Dependent Topographic Effects: A Case Study from the 1999 Athens Earthquake. *Earthquake Spectra*, 21 (4), pp. 929–966. doi: 10.1193/1.2068135.
- [23] Anbazhagan P, Sheikh MN & Parihar A (2013), Influence of rock depth on seismic site classification for shallow bedrock regions. *Natural Hazards Review*, 14 (2), pp. 108-121. doi: 10.1061/(ASCE)NH.1527-6996.0000088.
- [24] Adhikary S & Singh Y (2012), Effect of Soil Depth on Inelastic Displacement Spectra *Proc. 15 WCEE, Lisbon*.
- [25] D'Intinosante V, Baglione M & Gallori F (2016). La microzonazione sismica di terzo livello: l'esempio di Fivizzano ([http://www.ingenio-web.it/Articolo/4564/La\\_Microzonazione\\_Sismica\\_di\\_Terzo\\_Livello:\\_l\\_esempio\\_di\\_Fivizzano\\_%28MS%29.html](http://www.ingenio-web.it/Articolo/4564/La_Microzonazione_Sismica_di_Terzo_Livello:_l_esempio_di_Fivizzano_%28MS%29.html))
- [26] Tanganelli M, Viti S, Mariani V, Pianigiani M (2017). Seismic assessment of existing RC buildings under alternative ground motion ensembles compatible to EC8 and NTC 2008, *Bull Earthquake Eng* 15 (4), pp.1375–1396. doi: 10.1007/s10518-016-0028-z.
- [27] Tanganelli M, Viti S (2016). Effect of soil modeling on the seismic response of buildings. *Proc. SEMC 2016: Cape Town, South Africa, 5 - 7 September 2016*, Alphose Zingoni, vol. Insights and Innovations in Structural Engineering, Mechanics and Computation, pp. 284-290, ISBN:978-1-138-02927-9.
- [28] Pitilakis K, Riga E & Anastasiadis A (2013). New code site classification, amplification factors and normalized response spectra based on a worldwide earthquake database, *Bulletin of Earthquake Engineering*, 11(4), pp. 925–966. doi: 10.1007/s10518-013-9429-4.
- [29] NTC 2008. Norme tecniche per le costruzioni. D.M. Ministero Infrastrutture e Trasporti 14 gennaio 2008, G.U.R.I. 4 Febbraio 2008, Roma (in Italian).
- [30] Itaca [2008]. "Database of the Italian strong motions data". <http://itaca.mi.ingv.it>.
- [31] Iervolino I, Galasso C, Cosenza E (2009). REXEL: computer aided record selection for code-based seismic structural analysis. *Bulletin of Earthquake Engineering*, 8 (2), pp. 339-362. doi: 10.1007/s10518-009-9146-1.
- [32] Kramer SL (1996). *Geotechnical Earthquake Engineering*, Prentice-Hall, International Series in Civil engineering and engineering Mechanics, William J. Hall Editor.
- [33] Mazzoni S, McKenna F, Scott MH, Fenves GL (2009). *Open System for Earthquake Engineering Simulation, User Command-Language Manual*. (<http://opensees.berkeley.edu/OpenSees/manuals/usermanual>). Pacific Earthquake Engineering Research Center, University of California, Berkeley, OpenSees version 2.0.
- [34] Parra E (1996). Numerical modeling of liquefaction and lateral ground deformation including cyclic mobility and dilation response in soil systems." Ph.D. thesis, Rensselaer Polytechnic Institute, Troy, N.Y.
- [35] Yang Z, Elgamal A, Parra E (2003). A computational model for cyclic mobility and associated shear deformation. *Journal of Geotechnical and Geoenvironmental engineering (ASCE)*, 129 (12): pp. 1119-1127. doi: 10.1061/(ASCE)1090-0241(2003)129:12(1119).
- [36] Prevost, JH (1985). A simple plasticity theory or frictional cohesionless soils. *Soil Dynamics Earthquake Engineering*, 4 (1), pp. 9-17.
- [37] Dafalias YF (1986). Bounding surface plasticity I: mathematical formulation and hypoplasticity. *Journal of Engineering Mechanics*, ASCE 112 (9), pp. 966–987. doi: 10.1061/(ASCE)0733-9399(1986)112:9(966).
- [38] Bousshine L, Chaaba A, De Saxce G (2001). Softening in stress-strain curve for Drucker-Prager nonassociated plasticity. *International Journal of Plasticity* 17 (1), pp. 21–46. doi: 10.1016/S0749-6419(00)00017-6.
- [39] Nemat-Nasser S, Zhang J (2002). Constitutive relations for cohesionless frictional granular materials. *International Journal of Plasticity* 18 (4), pp. 531–547. doi: 10.1016/S0749-6419(01)00008-0.
- [40] Radi E, Bigoni D, Loret B (2002). Steady crack growth in elastic-plastic fluid-saturated porous media. *International Journal of Plasticity* 18 (3), pp. 345–358. doi: 10.1016/S0749-6419(00)00101-7.

- [41] Kondner RL (1963). Hyperbolic stress-strain response: Cohesive soils. *Journal of the Soil Mechanics and Foundations Division*, 89(SM1), pp. 115-143.
- [42] Law HK, Lam IP (2001). Application of periodic boundary for large pile group, *Journal of Geotechnical Geoenvironmental Engineering*, 127 (10), pp. 889–892. doi: 10.1061/(ASCE)1090-0241(2001)127:10(889).
- [43] Elgamal A, Lu J, Forcellini D (2009). Mitigation of Liquefaction-Induced lateral deformation in sloping stratum: Three-dimensional Numerical Simulation. *Journal of Geotechnical and Geoenvironmental Engineering* 135 (11), pp. 1672-1682. doi: 10.1061/(ASCE)GT.1943-5606.0000137.
- [44] Forcellini D, Gobbi S (2015). Soil structure interaction assessment with advanced numerical simulations, *Proceeding of Computational Method in Structural Dynamics and Earthquake Engineering conference (COMPDYN)*, Crete Island, 25 – 27 May 2015.
- [45] Forcellini D (2017). Cost Assessment of isolation technique applied to a benchmark bridge with soil structure interaction. *Bulletin of earthquake Engineering*. doi: 10.1007/s10518-016-9953-0.
- [46] Attewell, P. and Farmer, I.W. (1973), Attenuation of Ground vibrations from pile driving. *Ground engineering*, 6 (4), pp. 26-29.
- [47] Jesmani M, Fallahi AM, Kashani HF (2012). Effects of geometrical properties of rectangular trenches intended for passive isolation in sandy soils. *Earth Science Research* 1 (2), pp. 137-151. doi: 10.5539/esr.v1n2p137.
- [48] Forcellini D, Gobbi S, Mina D (2016). Numerical simulations of ordinary buildings with soil-structure interaction. VI International Conference on Structural Engineering, Mechanics and Computation (SEMC). Capetown, South Africa, 5-7 September 2016, ISBN 978-1-138-02927-9.
- [49] Elgamal A, Yang Z, Parra E and Ragheb A (2003). Modelling of cyclic mobility in saturated cohesionless soils. *International Journal Plasticity* 19 (6), pp. 883-905. doi: 10.1016/S0749-6419 (02)00010-4.